

Rapid Note

Weak surface energy in nematic dispersions: Saturn ring defects and quadrupolar interactions

O. Mondain-Monval^{1,a}, J.C. Dedieu², T. Gulik-Krzywicki², and P. Poulin¹¹ Centre de Recherche Paul Pascal - CNRS, avenue A. Schweitzer, 33600 Pessac, France² CGM-CNRS, avenue de la Terrasse, 91198 Gif-sur-Yvette, France

Received 21 June 1999

Abstract. The role of surface energy in the behavior of colloidal particles in liquid crystalline phases is investigated. When the surface energy dominates, a hedgehog defect is formed and, according to an electrostatic analogy, the distortions around the particles exhibit a dipolar character. By contrast, for weaker anchoring, the configuration becomes quadrupolar as evidenced by the structure of latex clusters in lyotropic systems and the observation of defects reminiscent of Saturn rings in thermotropic systems.

PACS. 61.30.Jf Defects in liquid crystals – 82.70.Dd Colloids – 83.70.Jr Liquid crystals: nematic, cholesteric, smectic, discotic, etc.

Liquid crystalline phases used as solvent for colloidal particles provide new ways of control over the spatial organization of colloidal systems. Well defined anisotropic structures and new phases have been recently observed in several systems such as mixtures of rod like viruses and colloids [1], molecular nematic emulsions [2], cholesteric dispersions [3] and suspensions of latex particles in micellar nematics [4,5]. Topological defects and distortions around the particles generate elastic forces that govern the stability and the ordering of the suspension. The particle surface properties impose the boundary conditions of the liquid crystal and the resultant far field distortions. Limits of so called strong anchoring were experimentally achieved in nematic solvent [2,5]. In such cases, the surface energy of the liquid crystal, of about wR^2 , largely dominates over the bulk elastic energy, of about KR , where w is a typical anchoring energy per unit surface, K a typical nematic elastic constant [6] and R the particle radius. As a main consequence, boundary conditions of the liquid crystal are fixed regardless the elastic energy of resultant distortions. For normal boundary conditions, the distortions exhibit a dipolar symmetry and particles tend to form chains aligned along the nematic director at infinity. For planar boundary conditions, the distortions exhibit quadrupolar symmetry, and the particles formed strings at an angle of 30° with respect to the director at infinity [2]. New behaviors can be expected if the surface energy becomes weaker. The liquid crystal may adopt different orientations at the interface of the particles in order to

partially relax the bulk elastic energy. In these conditions, different defects and distortions should take place; resulting in different spatial organizations of colloids in liquid crystals.

In this paper, we explore this limit of weak anchoring in systems where the ratio wR^2 over KR is lowered. Two different classes of composites are used: suspensions of latex particles in lyotropic liquid crystal and nematic emulsions consisting of water droplets suspended in thermotropic liquid crystal. In lyotropic dispersions, wR^2/KR is lowered using smaller particles. Freeze fracture and electron microscopy are used to analyze the colloidal structures that result from elastic interactions between nanometric particles. They form elongated clusters whose main axis adopts a non zero angle with respect to the director at infinity. This observation suggests that the particles experience quadrupolar interactions instead of dipolar ones [2]. Indeed, following an electrostatic analogy [7,8], two quadrupoles are expected to repel when aligned parallel or perpendicular to the nematic far field direction. By contrast, they attract each other along a direction that makes a finite angle between 0 and 90° with the director at infinity. In nematic emulsions, the ratio wR^2/KR is varied by changing the anchoring energy w through the use of different surfactant molecules adsorbed at the droplet interface. The liquid crystal distortions around micrometric droplets are observed using polarizing optical microscopy. The transition from dipolar to quadrupolar symmetry with decreasing anchoring energy is clearly confirmed by the observation of a disclination loop known as Saturn ring.

^a e-mail: mondain@crpp.u-bordeaux.fr

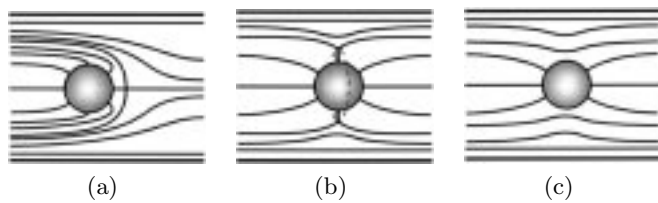


Fig. 1. Schematic of the director field around a colloidal particle in conditions of normal (or almost normal) boundary conditions: (a) Dipolar configuration with a hedgehog defect. (b) Quadrupolar configuration with a disclination loop (Saturn ring). (c) Quadrupolar configuration without topological defects in conditions of very weak anchoring.

Two possible configurations of a nematic liquid crystal around a particle are schematically drawn in Figures 1a and 1b, for a system with preferential normal boundary conditions. To satisfy the constraints that the liquid crystal is aligned far from the particle and normal to the particle surface (or almost normal for intermediate anchoring) a hedgehog defect (Fig. 1a) or a disclination loop (Fig. 1b) accompanies the particle. For very weak anchoring, a configuration without topological defects is theoretically expected [9] (Fig. 1c). Following an electrostatic analogy, the configuration with the hedgehog defect has dipolar symmetry whereas the system with the disclination loop and the configuration of Figure 1c have quadrupolar character. As experimentally [2,5] and theoretically [8–10] shown, the dipolar configuration is more stable in conditions of strong anchoring. As an important consequence, particles experience dipole-dipole interaction and form long chains aligned along the nematic director at infinity, as shown with water droplets in thermotropic liquid crystals [2] or with large latex particles (larger than 1 micron) in lyotropic discotic nematics [5].

Expecting a different behavior for smaller particles, we use 50 nanometers latex particles in similar discotic phases. The system is a micellar solution of cesium perfluorooctanoate (CsPFO, 53 weight %) in water including 2 weight % of particles. It has a phase sequence going from lamellar to nematic discotic, and isotropic phase with increasing temperature [4]. For the purpose of freeze fracture experiments, we use samples that contain 30 weight % of glycerol in water (glycerol is used as cryoprotectant to avoid the formation of ice crystals). Instead of arising from molecular interactions as in nematic emulsions, the anchoring is mainly due to entropic effects [5]; the excluded volume of the micelles being reduced when the disks are parallel to the interface [11]. This orientation leads to preferential normal boundary conditions for the director.

The latex particles remain dispersed in the nematic phase between 32 °C and 35 °C (the isotropic/nematic transition temperature). In this temperature range, the elastic constants and the anchoring are too weak to generate elastic interactions strong enough, with respect to the thermal energy $k_B T$, for a phase separation to take place. However, between 28 °C (the lamellar to nematic phase transition temperature) and 32 °C, the particles form a

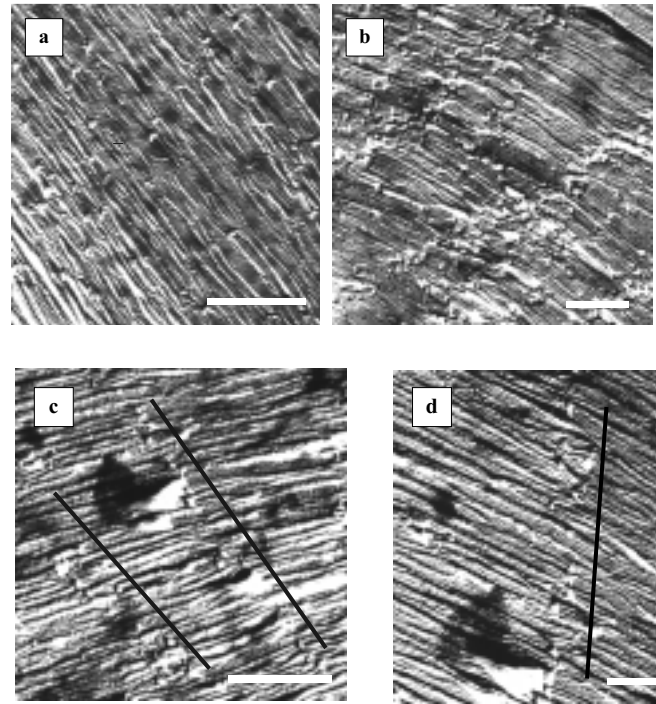


Fig. 2. Transmission electron microscope pictures of 50 nm latex particles in lyotropic nematic (CsPFO 53% in water/glycerol). The particles appear as white dots. The nematic director is normal to the observed stripes (bottom right corners: white bars corresponding to 500 nm). (a) Sample frozen from $T = 34$ °C. The particles are randomly dispersed in the nematic matrix. (b) Sample frozen from $T = 31$ °C. The particles form compact and elongated clusters. (c, d) Samples frozen from $T = 31$ °C. A few particles originating from the fracture of large initial aggregates allow identification of the cluster orientation with respect to the nematic director at infinity. Black lines parallel to the clusters are represented as guide to the eyes.

random texture [4] resultant from their aggregation in the nematic phase. Using freeze fracture-electron microscopy, this texture can be characterized at the nanometric scale. At 31 °C, the samples which exhibit the texture are deposited on Cu planchettes. They are afterward quenched rapidly by plunging them into liquid propane cooled to -190 °C by liquid nitrogen. The frozen samples are introduced into a vacuum chamber and fractured at a temperature of -150 °C. The replications are ensured by a shadowing of platinum, deposited at a 35° angle with respect to the fracture surface, followed by the deposition of a carbon film normal to the surface. The replicas are removed from the copper plate and cleaned in tetrahydrofuran to dissolve the latex particles. We observe the replica with a transmission electron microscope. We use the same procedure to observe samples frozen from $T = 34$ °C. As expected from the optical microscopy observations, the particles are aggregated at 31 °C (Figs. 2b–2d) whereas they are homogeneously dispersed at 34 °C (Fig. 2a). At 31 °C, the freeze fracture technique reveals a pronounced anisotropy of the texture which is not observed using

optical microscopy; the aggregates being elongated along a well defined direction. The anisotropy of the clusters is not due to the growth process in the anisotropic fluid. Instead, it is caused by anisotropic forces between the particles which are free to rearrange with respect to each other and to the nematic director in order to minimize the elastic energy. Although frozen from the nematic phase, the samples exhibit stripes which are usually observed in lamellar phases. Such stripes were also observed in samples free of particles. This means that the freezing step is long enough to allow local reorganization of the surfactant molecules from oblate micelles to extended bilayers. However, as shown by pictures of the high temperature sample (Fig. 2a), the latex particles are not affected by the quench. The surfactant bilayers resultant from the lateral fusion of the oblate micelles have their normal parallel to the initial nematic director. This allows the anisotropy of the latex clusters to be characterized with respect to the director. Instead of being aligned along the nematic director, the long axis of the clusters seems to adopt a non-zero angle with respect to the director. This effect is particularly clear in Figures 2c and 2d where the orientation of clusters is characterized by a few particles originating from large fractured aggregates.

The tilt from the normal suggests that the particles exhibit quadrupolar like behavior, in sharp contrast with the behavior of larger particles in the same discotic phase [5]. In order to confirm that the transition from dipolar to quadrupolar is due to weaker surface energy, we use nematic emulsions in which we can vary w .

Water-in-liquid crystal (inverted emulsion) or liquid crystal-in-water (direct emulsion) droplets are model systems because the anchoring can be controlled using various surfactants adsorbed at the liquid crystal-water interface. The nature and the energy of the anchoring is deduced by analyzing the internal configuration of liquid crystal droplets in water [12,13]. Although the curvature of the interface is opposite from inverted to direct systems, analysis of liquid crystal droplets is helpful to find systems with weaker anchoring. Indeed, anchoring is a molecular phenomenon which is not expected to strongly depend on the curvature of micrometric droplets interfaces which can be considered as flat at the molecular scale. To clearly analyze the internal configuration of liquid crystal droplets using optical microscopy we prepare large droplets of a few tens of microns. This is performed by gently shaking 5 weight % of liquid crystal (Merck E7) in an aqueous solution containing 1 weight % of a surfactant mixture composed of sodium dodecyl sulfate (SDS) and of a copolymer of ethylene and propylene oxide (Pluronic F 68). Depending on the ratio of SDS over F68 we find different patterns. Radial or bipolar configurations are observed when the SDS ratio is above roughly 25% or below 10%. These are respectively characteristic of strong normal and planar anchoring [12]. As shown in Figure 3a, between about 10 and 25%, equatorial configurations are observed. According to previous studies [12], these patterns indicate that weak normal boundary conditions are achieved in these latter conditions.

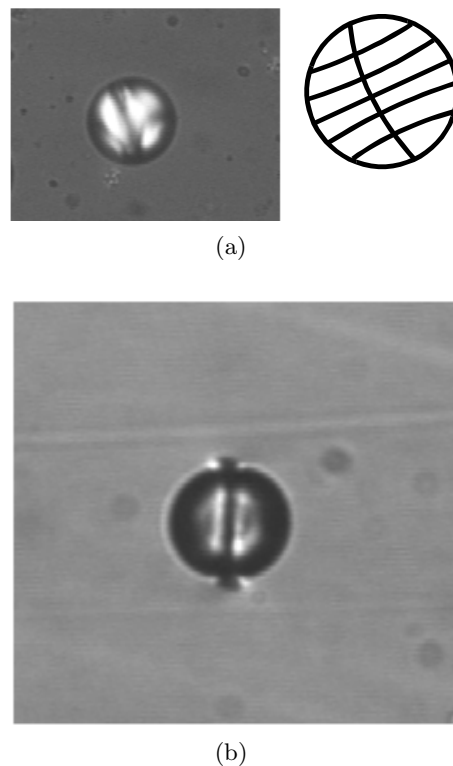


Fig. 3. (a) Optical microscope picture between crossed polarizers of a $20\ \mu\text{m}$ liquid crystal droplet in water (surfactant solution SDS: 0.20%; F68: 0.8%). The liquid crystal adopts an equatorial configuration with an internal disclination loop at the surface of the particle. The director field is sketched on the right schematic. This pattern results from weak normal anchoring. (b) Optical microscope picture of an equatorial ring around a $20\ \mu\text{m}$ water droplet (surfactant solution SDS: 0.20%; F68: 0.8%) in aligned nematic. Far field horizontal orientation of the director is provided by polymer coating and rubbing of the glass slides. The normal to the equatorial ring is aligned along the horizontal axis as sketched in Figure 1b.

Then we use these mixtures to determine the behavior of particles in liquid crystal by inverting the ratio of aqueous solution (5 weight %) over liquid crystal (95 weight %). Although the used surfactants are not efficient at stabilizing water droplets in organic solvent, the low concentration of water droplets allows isolated particles to be observed before they coalesce as they collide each other. As expected, when the SDS concentration is above 25% dipolar patterns with hedgehog defects, characteristic of strong normal anchoring, are observed. Below 10%, bipolar droplets with boojums defects, characteristic of strong planar anchoring, are observed. Both configurations are similar to those reported in literature [2]. As shown in Figure 3b, a new pattern consisting of an equatorial ring around the particle, is observed between 10 and 25%, in conditions of weaker anchoring. Such a ring provides quadrupolar symmetry to the system. We occasionally observe the coexistence of this pattern with hedgehog defects when the SDS ratio is close to 25%; meaning

that metastable states can coexist in particular anchoring conditions.

Theory [8] and computer simulations [9,10] show that a dipolar configuration is more stable in situation of strong anchoring. Exact calculations would be more complicated in the present case because the normal boundary constraints are relaxed due to weaker anchoring. However, a simple calculation can be proposed to compare the energetic cost of quadrupolar and dipolar configurations in conditions of very weak anchoring. In this limit, a particle can be suspended in the liquid crystal without accompanying defects but still with elastic distortions. Their energetic cost can be estimated using a single elastic constant [6]: $E_{el} = \int_v \frac{1}{2} K [(\text{div } \mathbf{n})^2 + (\text{curl } \mathbf{n})^2] dV$, where \mathbf{n} is the director field, aligned along the z axis at long range. Assuming multipolar fields [8] and considering the lowest order terms, we take $n_x = px/r^3$ and $n_y = py/r^3$ for the dipolar configurations and $n_x = qx/r^5$ and $n_y = qy/r^5$ for the quadrupolar configurations, where p and q are variational parameters and r the distance between the particle center and a point $M(x, y, z)$. The surface energy is calculated using the Rapini-Papoular expression [14]: $E_{surf} = \int_S \frac{1}{2} w (\sin \gamma)^2 dS$, where γ is the angle between the director and the surface normal. Minimizing $E_{surf} + E_{el}$ with respect to p and q gives the optimal configuration for a given size. In the limit of large K/wR , the energy of this optimum is lower for quadrupolar than for dipolar configurations. Since the dipolar configuration is more stable for infinite anchoring a transition is expected for intermediate value of weaker anchoring. We experimentally demonstrate that the expected crossover from dipolar to quadrupolar is achieved through the formation of an equatorial ring in thermotropics. In lyotropics, the defect structure is not elucidated but the shape and the orientation of the clusters reveal also quadrupolar symmetry. These findings agree well with recent simulations [9,10]. Note that the formation of a Saturn ring located at the surface of the particle is also expected [10,15]. It is nevertheless difficult to conclude from our pictures whether the observed equatorial ring corresponds to a disclination loop located at the surface or at a finite distance from the interface. Simulations predict metastability of the Saturn ring in conditions of strong anchoring. When lowering the anchoring, the ring energy is expected to decrease till it becomes lower than that of dipolar configuration. This expectation is in good agreement with the observed coexistence of equatorial rings and hedgehogs in conditions of weak anchoring. However, the absence of rings in conditions of strong anchoring indicates that the well depth and the energy barrier toward more stable dipoles are too low for Saturn rings to be observable. A second reason why Saturn rings are not observed for strong anchoring might be that they are not metastable at all.

The surface energy plays a determinant role in the behavior of particles suspended in liquid crystals. Varying this energy allows different colloidal structures to take place. As in classical suspensions in isotropic fluids, interactions between particles can be modulated by changing their surface chemistry. A unique feature of interactions in anisotropic fluids arises from the competition between bulk elastic and surface energy. This allows a control over the nature of interactions through particles size; this concept providing new possibilities to the tailoring of colloidal materials.

Stimulating and useful discussions with P. Barois, T.C. Lubensky, M. Zapotocky, P. Richetti, H. Stark and D.A. Weitz are gratefully acknowledged.

References

1. M. Adams, Z. Dogic, S.L. Keller, S. Fraden, *Nature* **393**, 349 (1998).
2. P. Poulin, H. Stark, T.C. Lubensky, D.A. Weitz, *Science* **275**, 1770 (1997); P. Poulin, D.A. Weitz, *Phys. Rev. E* **57**, 626 (1998).
3. M. Zapotocky, L. Ramos, P. Poulin, T.C. Lubensky, D.A. Weitz, *Science* **283**, 209 (1999).
4. P. Poulin, V.A. Raghunatan, P. Richetti, D. Roux, *J. Phys. II France* **4**, 1557 (1994); V.A. Raghunatan, P.D. Richetti, D. Roux, *Langmuir* **12**, 3789 (1996); V.A. Raghunatan, P. Richetti, D. Roux, F. Nallet, A.K. Sood, *Mol. Cryst. Liq. Cryst.* **288**, 181 (1996).
5. P. Poulin, N. Frances, O. Mondain-Monval, *Phys. Rev. E* **59**, 4384 (1999).
6. P.G. de Gennes, J. Prost, *The Physics of Liquid Crystals* (Oxford University Press, London, 1994).
7. S. Ramaswamy, R. Nityanada, V.A. Raghunathan, J. Prost, *Mol. Cryst. Liq. Cryst.* **288**, 175 (1996).
8. T.C. Lubensky, D. Pedey, N. Currier, H. Stark, *Phys. Rev. E* **57**, 610 (1998).
9. R.W. Ruhwandl, E.M. Terentjev, *Phys. Rev. E* **56**, 5561 (1997).
10. H. Stark, *Eur. Phys. J. B* **10**, 311 (1999).
11. A. Poniewierski, R. Holyst, *Phys. Rev. A* **38**, 3721 (1988).
12. P.S. Drzaic, *Liquid Crystal Dispersions*, Series on Liquid Crystals (World Scientific, Singapore, 1995), Vol. 1; S. Krajl, S. Zumer, *Phys. Rev. A* **45**, 2461 (1992); J.H. Erdmann, S. Zumer, J.W. Doane, *Phys. Rev. Lett.* **64**, 1907 (1990).
13. G.E. Volovik, O.D. Lavrentovich, *Sov. Phys. JETP* **58**, 1159 (1983).
14. A.A. Sonin, *The Surface Physics of Liquid Crystals* (Gordon and Breach, New York, 1995).
15. R.B. Meyer, *Solid St. Commun.* **12**, 585 (1973).